Received: 30 November 2020 | Revised: 22 January 2021 | Accepted: 29 January 2021

DOI: 10.1002/ardp.202000448

FULL PAPER

ARCH PHARM DPhG
Archiv der Pharmazie

# Synthesis and antitumor potential of new arylidene ursolic acid derivatives via caspase-8 activation

Baoen He[1] | Zuchang Zhu[1] | Fenglian Chen[1] | Rong Zhang[1] | Weiqiang Chen[2] | Te Zhang[3] | Tao Wang[1] | Jiamei Lei[1]

[1]School of Pharmaceutical Sciences, Guangzhou University of Chinese Medicine, Guangzhou, China

[2]School of Nursing, Guangzhou University of Chinese Medicine, Guangzhou, China

[3]Department of Research and Development, Shanghai Hequan Pharmaceutical Co. Ltd., Shanghai, China

**Correspondence**
Jiamei Lei and Tao Wang, School of Pharmaceutical Sciences, Guangzhou University of Chinese Medicine, Waihuan East Rd., No. 232, Guangzhou Higher Education Mega Center, 510006 Guangzhou, China.
Email: ljm123@gzucm.edu.cn and wangtao@gzucm.edu.cn

**Funding information**
Postdoctoral research from Guangzhou University of Chinese Medicine, Grant/Award Number: AFD01820Z0373

## Abstract

Continuing our studies on NO-donating ursolic acid–benzylidene derivatives as potential antitumor agents, we designed and synthesized a series of new arylidene derivatives containing NO-donating ursolic acid and aromatic heterocyclic units. Compounds **5c** and **6c** showed a significant broad-spectrum antitumor activity. Compound **5c** exhibited nearly three- to nine-fold higher cytotoxicity as compared with the parent drug in A549, MCF-7, HepG-2, HT-29, and HeLa cells, and it was also found to be the most potent apoptosis inducer of MCF-7 cells. More importantly, compound **5c** arrested the MCF-7 cell cycle in the G1 phase, which was associated with caspase activation and a decrease of the Bcl-2/Bax ratio. Meanwhile, compound **5c** caused changes in morphological features, dissipation of the mitochondrial membrane potential, and accumulation of reactive oxygen species. A docking study revealed that the nitroxyethyl moiety of compound **5c** may form hydrogen bonds with caspase-8 amino acid residues (SER256 and HIS255). Together, these data suggest that NO-donating ursolic acid–arylidene derivatives are potent apoptosis inducers in tumor cells.

**KEYWORDS**
antitumor activity, apoptosis inducer, NO donor prodrug, ursolic acid derivatives

## 1 | INTRODUCTION

Apoptosis (also called programmed cell death) was described to perform various functions in development.[1] It plays an important role not only in embryogenesis but also in the regulation of cell numbers and the elimination of unwanted cells. The previous literature pointed out that irregularity in apoptosis may cause a number of human diseases, such as neurodegenerative disorders, immunodeficiency, AIDS, and cancer.[2–4] Subsequent studies confirmed that apoptosis is one of the major pathways involved in the proliferation, migration, and invasion of tumor cells. Most of the cytotoxic compounds were reported to induce apoptosis in cancer cells. The developments of apoptosis inducers have become effective methods for cancer therapy.[5,6]

In general, there is a balance between apoptosis and proliferation in normal cells.[7] The balance depends on the Bcl-2/Bax ratio. It is worth noting that high levels of Bcl-2/Bax ratio may increase the risk of cancer. An excess of Bcl-2 promotes migration and invasion of tumor cells.[8] Morphological alterations, including cell shrinkage, chromatin condensation, and nuclear fragmentation, are important features of tumor cell apoptosis.[9] It has been proved that most of the morphological changes are caused by caspase family proteases. Caspases are divided into three subfamilies, I (caspase-2, -8, -9, and -10), II (caspase-3, -6, and -7), and III (caspase-1, -4, -5, -11, -12, -13, and -14).[10] Caspases I and II are involved in the activation and execution of apoptosis. During the process, initiator caspases activate downstream caspases, which are responsible for the cleavage of

Baoen He and Zuchang Zhu contributed equally to this study.

  

specific substrates and eventually cause apoptosis.[11] Currently, caspase-8 is considered as a key activator of apoptosis,[12] which can be activated by dimerization of procaspase-8 monomers.[13,14] The activation of caspase-8 may lead to stimulate caspase-3 and result in caspase protein cascade reaction.[15,16] Therefore, caspase-8 was considered as one of the major targets for cancer treatment. It is focused on by many pharmaceutical companies. However, the non-apoptotic functions of caspase-8 have also been gradually recognized in recent years.[17]

Ursolic acid (UA) is a ursane-type pentacyclic triterpene. As a ubiquitous chemical constituent derived from plants, UA exhibited an antitumor-promoting effect in vitro and in vivo.[18,19] Multiple molecular targets of UA have been proposed in many studies of antiproliferative mechanism, and most of them are related to apoptosis. Moreover, the reasonable modifications of the UA skeleton at positions 2, 3, and 28[20–22] have been found to increase antitumor activity and apoptosis induction. All of the above suggested that UA is an ideal starting point for the development of new antitumor agents.[23] The introduction of the Michael acceptor group in the parent structure is thought to improve the activity.[24,25] These active products are commonly obtained by using arylideneketones as convenient starting materials via Claisen–Schmidt condensation.[26] However, nitric oxide produced in large amounts by NO-releasing prodrug is known to mediate cytotoxicity. Thus, the design of NO-releasing prodrug has been a major topic of medicinal chemistry.[27,28]

Previously, we found that the hybrid compounds containing the NO-releasing UA scaffold linked to the Michael acceptor group exhibited a potent antitumor activity.[29] In this study, we describe further optimization for the design of NO-donating UA derivatives combined with heterocyclic aldehydes. The newly synthesized compounds were investigated for their antitumor activity against a panel of human tumor cell lines (A549, MCF-7, HepG-2, HT-29, and HeLa). Subsequently, a molecular docking study was carried out to clarify the binding mode between the most active compound and caspase-8. Finally, we intend to discover a new UA derivative as a potential apoptosis inducer via the caspase-8 activation.

## 2 | RESULTS AND DISCUSSION

### 2.1 | Chemistry

Heterocyclic compounds have been reported to possess a wide range of biological activities, including antibacterial, antitumor, anti-inflammatory, and anticonvulsant effects. The synthesis, the physical properties, and the biological activities of hybrid compounds containing different heterocyclic fragments have been widely investigated.[30–33] Motivated by these findings, we designed and synthesized new arylidene UA derivatives incorporating oxygen-, sulfur-, and nitrogen-containing heterocycles. Furan, thiophene, pyridine, and pyrimidine derivatives were reported to have antitumor activity.[34–36] Therefore, we designed the synthetic route of UA hybrid molecules containing heterocyclic moieties mentioned above. The target compounds were prepared according to the reactions outlined in Scheme 1.

First, it is necessary to prepare an active methylene intermediate **2** for the introduction of heterocyclic moieties. Second, Claisen–Schmidt condensation of **2** with different heterocyclic formaldehyde (furaldehyde, 2-thenaldehyde, 4-pyridylaldehyde, and 4,6-dimethoxypyrimidine-5-carbaldehyde) was carried out in

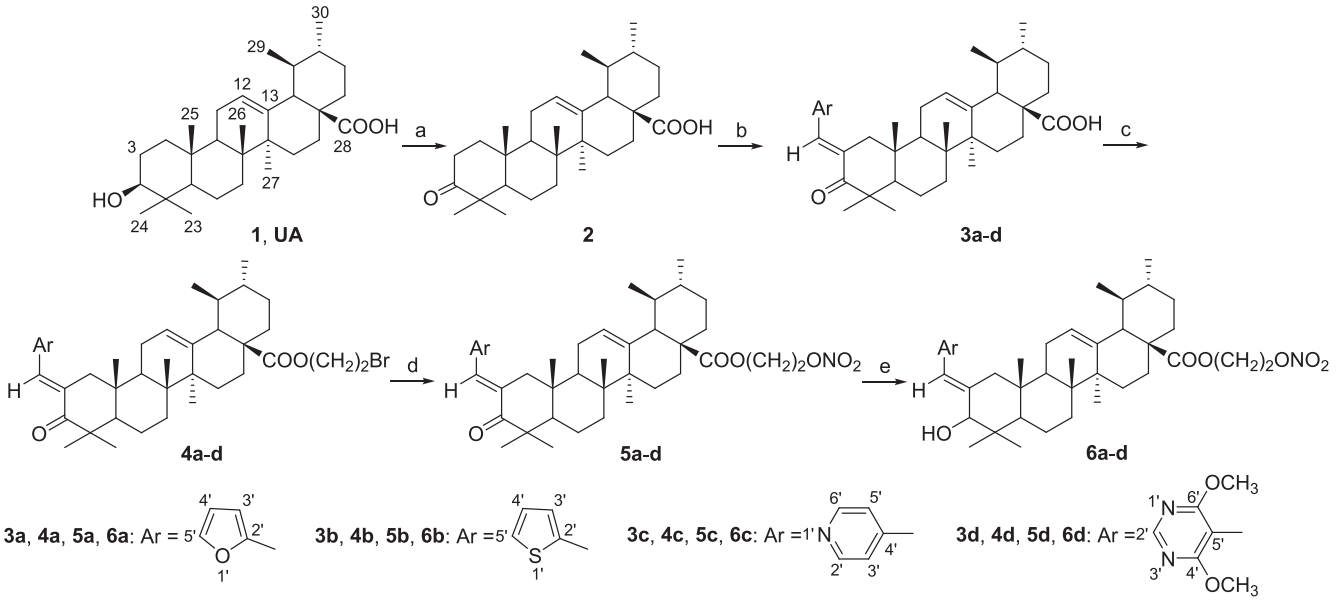


**SCHEME 1** Synthesis of NO-donating ursolic acid derivatives containing heterocyclic moieties **5a–d** and **6a–d**. Reagents and conditions: (a) Dess–Martin periodinane, $CH_2Cl_2$, rt, 6 h; (b) aromatic aldehydes, EtOH, KOH, rt, 5–24 h; (c) $Br(CH_2)_2Br$, DMF, $K_2CO_3$, rt, 12 h; (d) $AgNO_3$, $CH_3CN$, 50°C, 24 h; (e) $NaBH_4$, THF + EtOH, rt, 2 h

ethanol under base catalysis, as described in our previous paper.[29] NO-donating UA derivatives **5a–d** containing heterocyclic moieties were synthesized via two-step nucleophilic substitution, which has been widely used in the preparation of organic nitrate prodrugs. Compounds **5a–d** were reduced with sodium borohydride in tetrahydrofuran (THF) to give another series of NO-donating UA derivatives containing heterocyclic moieties **6a–d**. All of the target compounds were purified by silica gel column chromatography. Then, their structures were confirmed by infrared (IR), nuclear magnetic resonance (NMR), and high-resolution mass spectrometry (HRMS).

All spectral data were consistent with the proposed structure. The characteristic IR absorption bands of OH, C═O, C═C, and C–O–C were observed at ~3557, ~1669 to 1730, ~1637, and ~1280 $cm^{-1}$, respectively. Furthermore, the data of NMR provided strong support for the existence of heterocyclic moieties and the formation of nitroxyethyl. The proton signals at $\delta$ ~4.65 and ~4.28 ppm indicated the presence of two methylene groups in nitroxyethyl. The proton signals of heterocyclic and methyl groups in the UA ring were also found in the expected region. We found that a new proton signal emerged at ~3.85 ppm after reduction of the C-3 carbonyl group. In addition, the chemical shifts of methylene carbon in heterocyclic appeared at 101.2–167.6 ppm. The signals (~70.6 and ~60.2 ppm) were assigned to the methylene carbon of nitroxyethyl.

## 2.2 | Antitumor activity

It is well known that sulforhodamine B (SRB), 3-(4,5-dimethylthiazol-2-yl)-2,5-diphenyltetrazolium bromide (MTT), and cell-counting kit-8 (CCK-8) assays are used infrequently for in vitro anticancer drug screening. Previous studies demonstrated that the results of the MTT test are well correlated with those of the SRB assay. To ensure the reliability of the results, these two methods have always been used simultaneously to determine cell viability.[37] However, several studies reported that MTT and CCK-8 assay exhibited inconsistent results.[38] It is important to note that we need to select the suitable method of cell viability based on its advantages and scope of application. Considering that MTT assay is generally applied to measure the proliferation of adherent cells,[39] we chose this method for evaluation of the antiproliferative activity.

All new compounds, **5a–d** and **6a–d**, were screened for their in vitro antitumor activity against five human tumor cells: A549, MCF-7, HepG-2, HT-29, and HeLa cells. As control groups, a culture medium, a culture medium containing 0.1% dimethyl sulfoxide (DMSO), UA, and cisplatin were used in the experiment. We determined cell viability after tumor cell lines were treated with various concentrations of test compounds for 48 h. The mean $IC_{50}$ values of the compounds are shown in Table 1.

It is clear that UA displayed a considerable inhibitory activity in vitro against all tested tumor cell lines, with $IC_{50}$ values ranging from 40.28 μM to 66.53 μM. The viability of all cell lines was not inhibited by thiophene-containing NO-donating UA derivatives **5b** and **6b** at 100 μM maximum concentration. Interestingly, furan-containing and pyrimidine-containing derivatives **5a**, **6a**, and **6d** were found to exhibit selective inhibition against different tumor cell lines. Moreover, pyridine-containing NO-donating UA derivatives **5c** and **6c** showed a significant broad-spectrum antitumor activity. The inhibitory effect was exerted in a dose-dependent manner. Compound **5c** displayed three- to nine-fold greater inhibitory activity against five tumor cell lines as compared with UA. Among all the tumor cell lines tested, MCF-7 was found to be most sensitive to compound **5c**. Further study of apoptosis was investigated using only this cell line. The results of the cytotoxic evaluation indicated that the introduction of pyridine structure into the UA skeleton may improve the antitumor activity. In addition, the presence of the carbonyl group at the C3 position is necessary for the inhibitory effect.

**TABLE 1** $IC_{50}$ values (μM) of UA derivatives **5a–d** and **6a–d** against different tumor cell lines

| | $IC_{50}$ (μM) | | | | |
|---|---|---|---|---|---|
| Compound | Lung cancer A549 | Breast cancer MCF-7 | Liver cancer HepG-2 | Colon cancer HT-29 | Cervical cancer HeLa |
| **5a** | 24.45 ± 0.06 | >100 | >100 | >100 | >100 |
| **5b** | >100 | >100 | >100 | >100 | >100 |
| **5c** | 7.96 ± 0.61 | 7.42 ± 0.51 | 13.35 ± 0.18 | 12.99 ± 0.02 | 17.05 ± 0.06 |
| **5d** | >100 | >100 | >100 | >100 | >100 |
| **6a** | >100 | 14.48 ± 0.44 | >100 | 43.88 ± 0.86 | >100 |
| **6b** | >100 | >100 | >100 | >100 | >100 |
| **6c** | 13.77 ± 0.28 | 12.74 ± 1.10 | 20.13 ± 0.44 | 17.21 ± 0.36 | 33.44 ± 1.08 |
| **6d** | >100 | 13.96 ± 0.05 | >100 | >100 | >100 |
| **1** | 45.36 ± 0.84 | 66.53 ± 1.03 | 43.25 ± 0.45 | 40.28 ± 0.56 | 56.30 ± 0.44 |
| Cisplatin | 22.23 ± 0.04 | 23.06 ± 0.12 | 22.42 ± 0.12 | 13.44 ± 0.10 | 8.67 ± 0.03 |

*Note*: $IC_{50}$ values are the mean ± *SD* of three individual experiments determined after 48-h treatment. Cisplatin is a positive control.

## 2.3 | Apoptosis detection

### 2.3.1 | Morphological changes detection

Apoptosis is known as a common mode of death in many tumor cells. As described previously, the apoptotic process of cells was accompanied by morphological changes.[40] Light microscopy, electron microscopy, and DNA electrophoresis analysis are powerful tools in the analysis of morphological changes in apoptotic cells.[41] Fluorescent staining techniques, which can identify apoptotic changes in the nucleus, are widely applied to measure the apoptosis of tumor cells in recent years.[42] Here, 4′,6-diamidino-2-phenylindole (DAPI) and acridine orange/ethidium bromide (AO/EB) staining were used to observe morphological changes characteristic of apoptosis in the MCF-7 cells.

The staining results are shown in Figure 1. DAPI is a DNA-specific fluorescent dye, which can stain nuclei of tumor cells as blue spots. During apoptosis of tumor cells, cell membrane integrity was lost and subsequent apoptotic characteristics appeared. Images of DAPI staining revealed that the cells of the control group possess large-volume nuclei and intact membrane. After MCF7 cells were treated with compound **5c**, nuclei pyknosis and DNA fragmentation were found (Figure 1a). The occurrence of apoptosis induced by compound **5c** was preliminary confirmed. The results were further substantiated by AO/EB staining. AO/EB staining is another useful detection of changes in nuclei.[43] Many publications have reported that live cells with intact membrane were stained green by AO. Late apoptotic cells were stained orange by EB when their membrane integrity was lost. The same results were found in our study (Figure 1b). These findings suggested that low concentrations of compound **5c** induced early apoptosis in MCF-7 cells, whereas high concentrations of compound **5c** mainly induced late apoptosis.

### 2.3.2 | Apoptosis and cell cycle detection

To quantitatively determine apoptosis of MCF-7, annexin V-fluorescein isothiocyanate (FITC)/propidium iodide (PI) staining was performed in our study. Annexin V has a high affinity for phosphatidylserine. Translocation of membrane phosphatidylserine was found at the early stage of apoptosis. Hence, FITC-labeled annexin V can be used for the detection of early-stage apoptosis using flow cytometry. Once cells entered the late-stage apoptosis, apoptotic nuclei were stained by PI due to the disappearance of cell membranes integrity. It is indicated that the different stages of apoptotic cells can be distinguished by the combination of annexin V-FITC and PI.[44] As shown in Figure 2a, the proportion of early and late apoptotic cells was increased in a dose-dependent manner. We also found that late-stage apoptosis predominated at $2 \times IC_{50}$ concentration of compound **5c**.

Mammalian development and homeostasis are dependent on the regulation of apoptosis and the cell cycle.[45] It has been believed that progression through the different phases of the cell cycle is governed by the cyclin-dependent kinases (Cdks).[46] Different Cdks functioned at specific stages during cell cycle progression.[47] Therefore, targeting the cell cycle provides a valuable strategy for the inhibition of tumor cell proliferation.[48] Previous evidence has shown that antitumor agents mainly arrested cell cycle at S and G1 phases.[49] To investigate the effects of compound **5c** on the cell

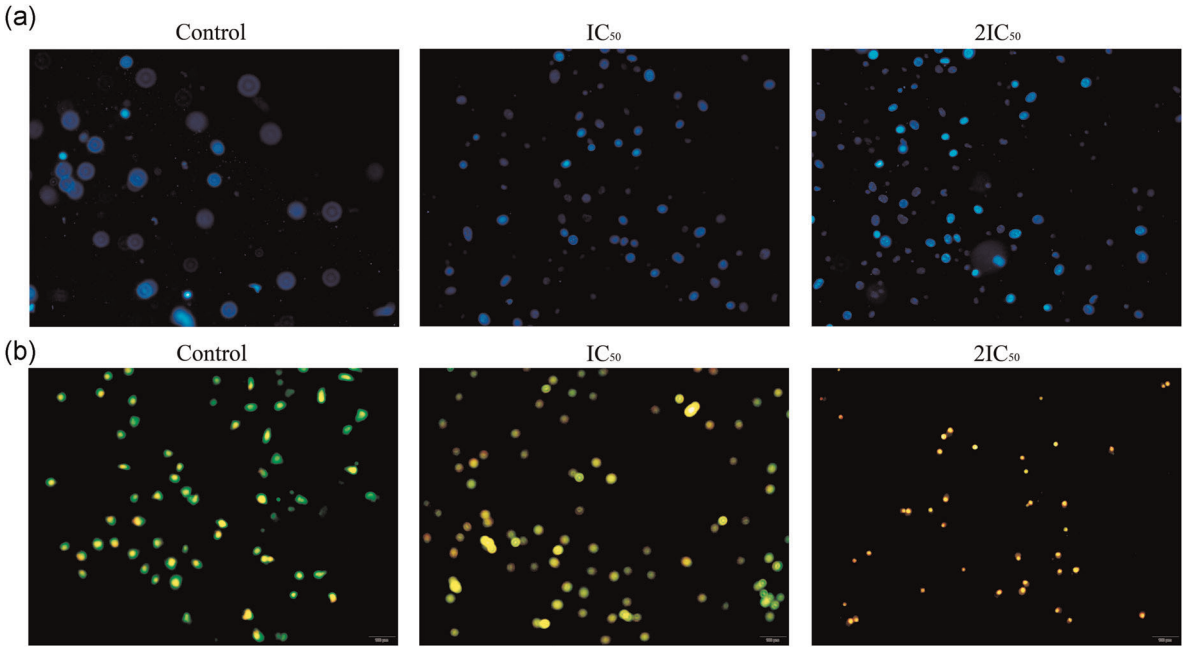


**FIGURE 1** Cellular morphologic observation of MCF-7 after treatment with different concentrations of compound **5c** (0, $IC_{50}$, and $2IC_{50}$). (a) 4′,6-Diamidino-2-phenylindole staining; (b) acridine orange/ethidium bromide staining

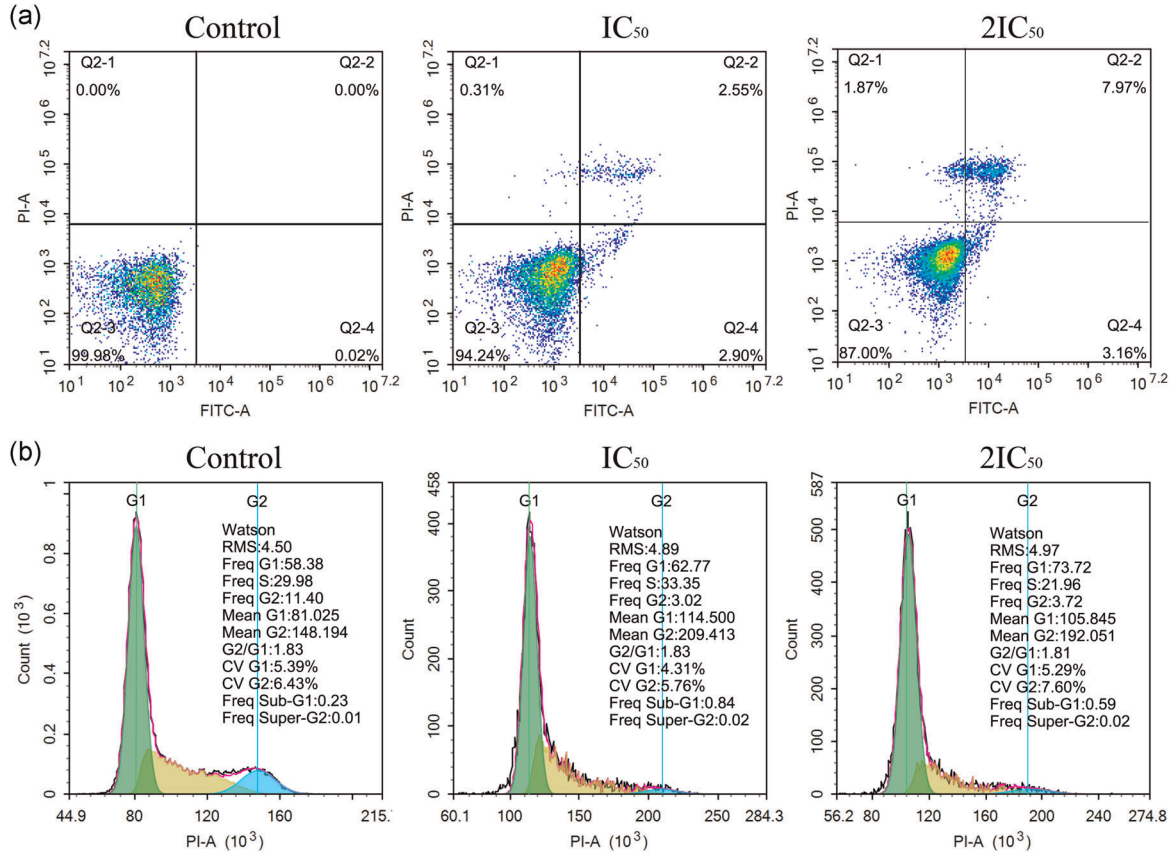


**FIGURE 2** Apoptosis and cell cycle assay of compound **5c** on MCF-7. (a) Cells were treated with different concentrations of compound **5c** (0, $IC_{50}$, and $2 \times IC_{50}$) for 24 h, stained with annexin V-FITC/PI, and observed by flow cytometry; (b) cells were treated with different concentrations of compound **5c** (0, $IC_{50}$ and $2 \times IC_{50}$) for 24 h, stained with PI, and observed by flow cytometry. FITC, fluorescein isothiocyanate; PI, propidium iodide

cycle of MCF-7 cells, the cell cycle was determined by staining DNA with PI and flow cytometry. Figure 2b indicated that compound **5c** caused an increase of the G1 phase cell population and a decrease of the G2 phase cell population after 24 h of treatment. A dose-dependence effect on the cell cycle was also observed. Multiple studies have confirmed that DNA replication is initiated in the G1 phase. The tumor suppressor p53 is involved in G1 phase arrest and induction of apoptosis.[50] These facts give a good reason for us to speculate that compound **5c** induced G1 phase arrest via regulating p53 expression in MCF-7 cells.

### 2.3.3 | Membrane potential and reactive oxygen species (ROS) detection

To date, both ROS and mitochondria involved in apoptosis induction have been recognized. ROS are considered as an effective activator of mitochondrial permeability transition pore (MPTP) opening. The loss of mitochondrial membrane potential is observed after the irreversible opening of MPTP.[51] This is accompanied by the release of cytochrome *c*, activation of caspase cascades, and ultimately apoptosis. All this evidence suggests that the loss of mitochondrial membrane potential is one early hallmark of apoptosis.[52] In the present study, ROS level and membrane potential were measured by using flow cytometry simultaneously.

JC-1 probe has been frequently used to monitor mitochondrial potential due to its fluorescent properties depending on membrane potential. When the mitochondrial membrane potential changed, the transition between JC-1 dye monomer and J-aggregates resulted in a fluorescence shift from green to red. The results of mitochondrial membrane potential analysis are shown in Figure 3a and displayed as an image composed of four quadrants. JC-1 monomer accumulated in control cells and exhibited a high ratio of green fluorescence. After treatment with different concentrations of compound **5c**, the red/green ratio in Q3 quadrants increased to 14.9%, and 20.7%, respectively. The results indicated that the apoptosis of MCF-7 induced by compound **5c** was associated with mitochondrial membrane depolarization and was carried out in a dose-dependent manner.

A previous study has pointed out that ROS are involved in different pro- and anticarcinogenic mechanisms.[53] A moderate increase in ROS can promote cell proliferation and differentiation. However, a high level of ROS tends to inhibit tumor cell growth and induce apoptosis.[54] The overproduction of ROS may lead to

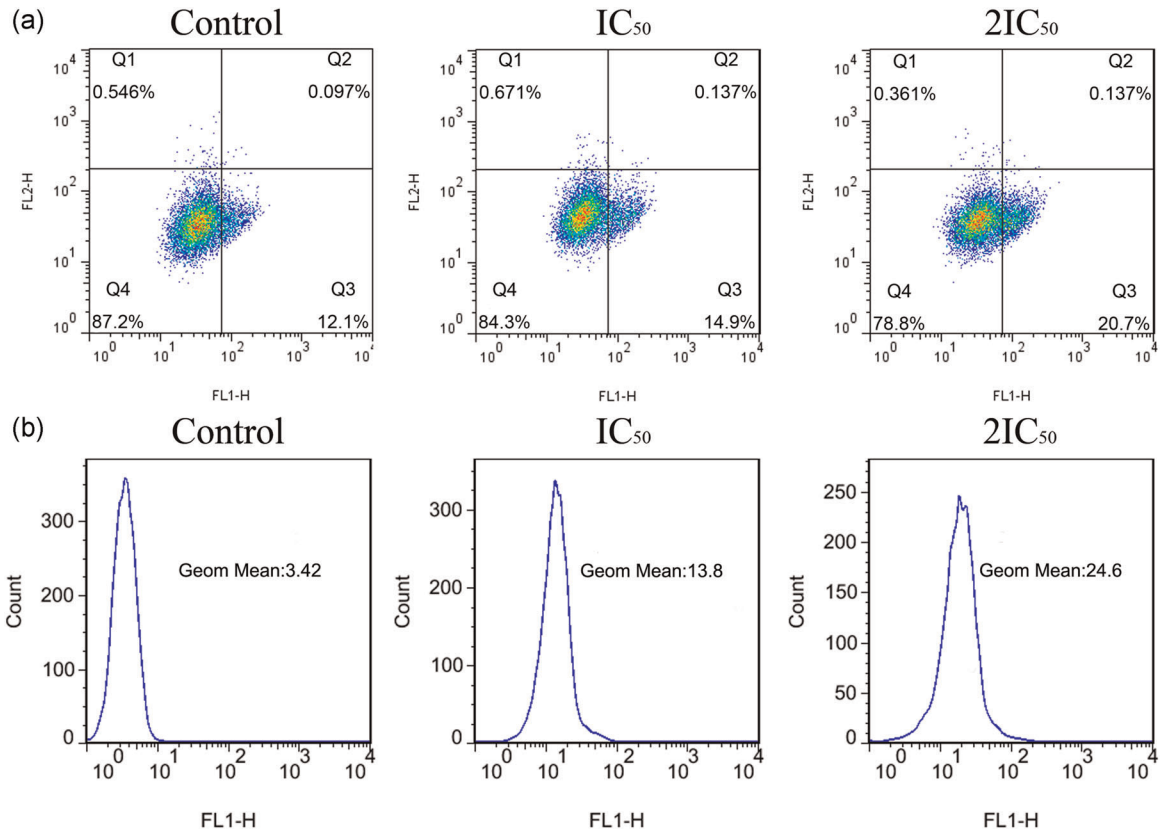


**FIGURE 3** Membrane potential and reactive oxygen species assay of compound **5c** on MCF-7. (a) Cells were treated with different concentrations of compound **5c** (0, $IC_{50}$ and $2 \times IC_{50}$) for 24 h, stained with JC-1, and determined by flow cytometry; (b) cells were treated with different concentrations of compound **5c** (0, $IC_{50}$, and $2 \times IC_{50}$) for 24 h, stained with 2′,7′-dichlorofluorescein diacetate, and analyzed by flow cytometry

oxidative stress, which can cause damages in DNA, proteins, and lipids. Numerous investigations have documented that many chemotherapeutic drugs induce apoptosis by increasing ROS production. To confirm the effect of compound **5c** on ROS in MCF-7 cells, the level of ROS was tested by 2′,7′-dichlorofluorescein diacetate (DCFH-DA). After the penetration of DCFH-DA into the cell membrane, it was hydrolyzed by intracellular esterase to DCFH. Further oxidization of DCFH by ROS produced DCF, which is a highly fluorescent compound. Many studies have found that there is a quantitative relationship between the DCF fluoresce intensity and the amount of ROS.[55] Figure 3b showed that the level of ROS in treated groups notably increased to 13.8% and 24.6% as compared with that in the control group (3.42%). These results demonstrated that compound **5c** could increase the level of ROS in a dose-dependent manner. So, we infer that ROS production may be a possible mechanism for apoptosis induction of MCF-7 cells by compound **5c**.

### 2.3.4 | Western blot analysis

It is widely recognized that most anticancer drugs induce apoptosis through the mitochondrial pathway. Mitochondrial membrane potential plays an important role in maintaining the normal function of mitochondria. A number of previous reports have indicated that the loss of the mitochondrial membrane potential was associated with the Bcl-2 (antiapoptotic protein)/Bax (proapoptotic protein) ratio.[56,57] Subsequently, the release of cytochrome *c* and activation of caspases cascade were observed.[58] Therefore, we investigated a number of key protein markers by the Western blot analysis. The results of the Western blot analysis are shown in Figure 4. After treatment with different concentrations of compound **5c**, the expression of Bax, caspase 3, and caspase 9 was remarkably upregulated. Besides, Bcl-2 expression was downregulated in MCF-7 cancer cells. It is reasonable to presume that compound **5c** induces apoptosis of MCF-7 tumor cells through regulating the Bcl-2/Bax ratio, leading to the loss of the mitochondrial membrane potential and activation of caspases.

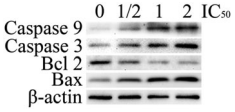


**FIGURE 4** The results of Western blot analysis of compound **5c** on MCF-7 cells. Cells were treated with different concentrations of compound **5c** (0, $0.5 \times IC_{50}$, $IC_{50}$ and $2 \times IC_{50}$) for 24 h and total protein was extracted to determine the expression of caspase-9, caspase-3, Bcl 2, and Bax

## 2.4 | Molecular docking studies

Caspase-8 is one of the critical initiators of apoptosis. Apoptosis induced by anticancer drugs is mediated by the activation of caspase-8 in many tumor cells. It has also been found that caspase-8 may serve as an amplifier of apoptotic signals.[59] Thus, targeting caspase-8 to initiate apoptosis may offer a promising therapeutic opportunity in cancer. Here, the further study on the docking interactions of potent compound and caspase-8 was performed by computational analysis. The binding mode of compound **5c** and caspase-8 was studied by docking and is presented in Figure 5. On the basis of the total score of 7.31, compound **5c** showed an excellent interaction within the 2c2z protein pocket of caspase-8. The two-dimensional docking interaction between compound **5c** and caspase-8 active site is presented in Figure 5a. It should be noted that pi–alkyl interactions were colored in pink, whereas the hydrophobic interactions were colored in green. As seen in Figure 5a, pi–alkyl interactions were found between the UA skeleton of compound **5c** and residues of caspase-8, including CYS360, VAL410, ARG258, HIS317, and ILE257, wherein the pi–alkyl distances ranged from 2.06 Å to 4.01 Å. Moreover, SER256 and HIS255 residues of caspase-8 are engaged in additional hydrophobic interactions with nitroxyethyl moiety (distances: 1.93 Å and 2.26 Å). Figure 5ab showed that nitroxyethyl moiety of compound **5c** docked into the hydrophobic pocket of caspase-8. It might be assumed that the 2c2z-pocket of caspase-8 participates in the apoptotic regulation by acting as a docking site for substrates.

## 3 | CONCLUSION

In recent years, pentacyclic triterpenoids have received much attention as lead compounds for the development of the new antitumor drug. Lupane-, oleanane-, and ursane triterpenoids are particularly prominent among the known research. In view of the antitumor effects of pentacyclic triterpenoids and their semisynthetic derivatives, we synthesized eight new arylidene derivatives containing NO-donating UA and aromatic heterocyclic units. In vitro evaluation against five tumor cell lines (A549, MCF-7, HepG-2, HT-29, and HeLa cells) and molecular recognition were undertaken.

The MTT assay showed that pyridine-containing NO-donating UA derivatives **5c** and **6c** exhibited a broad spectrum of antitumor activity, with $IC_{50}$ values better than those of the parent compound (UA). Compound **5c** was the most active derivative against MCF-7 cells ($IC_{50}$ 7.42 μM). A preliminary mechanism of antitumor activity demonstrated that the cytotoxicity of compound **5c** against MCF-7 cells may be related to the decrease of mitochondrial membrane potential, the increase in the level of ROS, and cell cycle arrest in the G1 phase to induce apoptosis. The expression of key protein markers hinted that compound **5c** induced MCF-7 cells apoptosis in a mitochondrial-dependent manner. Moreover, compound **5c** effectively interacted with the active site of caspase 8 via hydrogen bonds. Our results indicated that compound **5c** may be a promising anticancer agent worthy of further study.

## 4 | EXPERIMENTAL

### 4.1 | Chemistry

#### 4.1.1 | General

All chemicals and reagents were obtained from commercial suppliers. When necessary, reagents were dried and purified before use. All reactions were monitored by thin-layer chromatography (TLC) on silica gel GF254 plates and spots were visualized with 5% vanillin–sulfuric acid. Melting points were measured on the X-6 microscopic melting point apparatus and were uncorrected. IR spectra were obtained on a Nicolet 330 FT-IR spectrometer. NMR spectra were determined in $CDCl_3$ on a Bruker Avance spectrometer (400 MHz for $^1H$ NMR, 100 MHz for $^{13}C$ NMR). High-resolution mass spectra were recorded on an AB SCIEX Triple TOF™ 5600$^+$ LC-MS/MS system. The original spectra can be found in the Supporting Information.

The InChI codes of the investigated compounds, together with some biological activity data, are provided as Supporting Information.

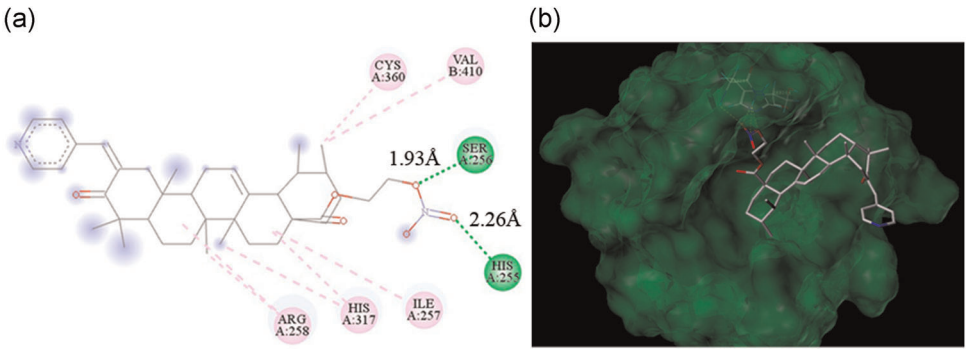


**FIGURE 5** Docking interaction between compound **5c** and caspase-8 (PDB: 2c2z). (a) Two-dimensional structure of compound **5c** docked into the caspase-8 active site; (b) three-dimensional conformation of compound **5c** bound to caspase-8 interface region

### 4.1.2 | General procedure for the preparation of intermediates **2, 3a–d, 4a–d**, and compounds **5a–d**

The intermediates were synthesized as described in Reference [29] .UA **1** (1 eq.) was dissolved in dichloromethane and subjected to oxidation by Dess–Martin periodinane (1 eq.) to give compound **2**. The condensation of compound **2** (1 eq.) with various aromatic aldehydes (1–1.5 eq.), namely, furaldehyde, 2-thenaldehyde, 4-pyridylaldehyde, and 4,6-dimethoxypyrimidine-5-carbaldehyde, in ethanol and in the presence of a base, afforded compounds **3a–d**. Compounds **4a–d** were obtained by stirring of compounds **3a–d** (1 eq.) with 1, 2-dibromoethane (4–8 eq.) at room temperature for 12 h in 41–73% yields. Finally, silver nitrate (10–12 eq.) was added to a solution of compounds **4a–d** (1 eq.) in acetonitrile. The mixture was heated at 50°C for 24 h. The products **5a–d** were prepared as yellow or yellow-white or yellow-green solids.

*2-[2-(Furan-2-yl)vinyl]-3-oxo-urs-12-en-28-oic acid-(2-nitrooxy)-ethyl ester (**5a**)*

Yellow solid; yield 90.3%; m.p. 123.3–123.9°C; IR (KBr): $\tilde{\nu}$ = 2924 (vs), 2869 (m) (C–H, aliphatic), 1730 (s), 1672 (m) (2C=O), 1637 (vs) (C=C), 1594 (m), 1542 (w), 1455 (m) (C=C, furanyl), and 1280 (vs) (C–O–C, ester) $cm^{-1}$; $^1H$ NMR (400 MHz, $CDCl_3$): $\delta$ = 0.80, 0.90, 1.10, 1.14, 1.16 (15H, s, 5× $CH_3$), 0.92, 0.96 (6H, d, $J$ = 6.4, 6.2 Hz, 2× $CH_3$), 4.30 (2H, m, –$OCH_2$), 4.65 (2H, m, $CH_2ONO_2$), 5.34 (1H, t, $J$ = 7.0, 3.3 Hz, H-12), 6.51 (1H, m, 4'-H), 6.61 (1H, d, $J$ = 3.4 Hz, 3'-H), 7.33 (1H, s, =CHAr), and 7.57 (1H, d, $J$ = 1.6 Hz, 5'-H) ppm; $^{13}C$ NMR (100 MHz, $CDCl_3$): $\delta$ = 15.9 (C30), 16.8 (C29), 17.2 (C27), 20.5 (C6), 21.3 (C23), 22.7 (C26), 23.5 (C24), 23.8 (C11), 24.2 (C16), 28.0 (C21), 30.0 (C25), 30.7 (C15), 32.2 (C1), 35.8 (C10), 36.7 (C22), 39.0 (C20), 39.3 (C19), 39.5 (C8), 42.6 (C14), 44.4 (C7), 45.0 (C17), 45.3 (C9), 48.5 (C4), 52.9 (C18), 53.2 (C5), 60.2 ($COOCH_2$), 70.7 ($CH_2ONO_2$), 112.4 (C3'), 115.7 (C4'), 124.4 (=CHAr), 125.9 (C12), 130.9 (C13), 138.2 (C2), 144.5 (C5'), 152.7 (C2'), 177.3 (C28), and 207.3 (C3) ppm; HRMS ($m/z$) $[M+H]^+$ calcd. for $C_{37}H_{52}NO_7$: 622.3738, found: 622.3733.

*2-[2-(Thiophene-2-yl)vinyl]-3-oxo-urs-12-en-28-oic acid-(2-nitrooxy) ethyl ester (**5b**)*

Yellow solid; yield 70.3%; m.p. 127.4–128.2°C; IR (KBr): $\tilde{\nu}$ = 2949 (vs), 2869 (m) (C–H, aliphatic), 1729 (s), 1669 (m) (2C=O), 1636 (vs) (C=C), 1579 (m), 1455 (m) (C=C, thiopheneyl), and 1280 (vs) (C–O–C, ester) $cm^{-1}$; $^1H$ NMR (400 MHz, $CDCl_3$): $\delta$ = 0.80, 0.91, 0.94, 0.96, 1.10, 1.14, 1.18 (21H, s, 7× $CH_3$), 4.31 (2H, m, –$OCH_2$), 4.65 (2H, m, $CH_2ONO_2$), 5.36 (1H, t, $J$ = 7.0, 3.3 Hz, H-12), 7.14 (1H, q, $J$ = 5.1, 3.7 Hz, 4'-H), 7.32 (1H, d, $J$ = 3.5 Hz, 5'-H), 7.51 (1H, d, $J$ = 5.1 Hz, 3'-H), and 7.74 (1H, s, =CHAr) ppm; $^{13}C$ NMR (100 MHz, $CDCl_3$): $\delta$ = 16.0 (C29), 16.8 (C30), 17.2 (C23), 20.6 (C6), 21.3 (C24), 22.7 (C27), 23.6 (C26), 23.7 (C11), 24.3 (C22), 28.0 (C21), 30.1 (C25), 30.7 (C7), 32.2 (C16), 36.2 (C10), 36.7 (C15), 39.0 (C19), 39.3 (C20), 39.6 (C8), 42.4 (C17), 44.8 (C1), 45.0 (C14), 45.6 (C18), 48.5 (C4), 52.8 (C9), 53.1 (C5), 60.2 ($COOCH_2$), 70.7 ($CH_2ONO_2$), 125.9 (C12), 127.7 (C3'), 129.8 (C4'), 130.5 (C5'), 130.8 (C2'), 132.8 (=CHAr), 138.1 (C13), 139.6 (C2), 177.3 (C28), and 207.4 (C3) ppm; HRMS ($m/z$) $[M+H]^+$ calcd. for $C_{37}H_{52}SNO_6$: 638.3510, found: 638.3504.

*2-[2-(Pyridin-4-yl)vinyl]-3-oxo-urs-12-en-28-oic acid-(2-nitrooxy)-ethyl ester (**5c**)*

Yellow-white solid; yield 55.5%; m.p. 113.9–114.5°C; IR (KBr): $\tilde{\nu}$ = 2924 (vs), 2869 (m) (C–H, aliphatic), 1728 (s), 1669 (m) (2C=O), 1636 (vs) (C=C), 1455 (m), 1579 (m) (C=N, pyridinyl), and 1280 (vs) (C–O–C, ester) $cm^{-1}$; $^1H$ NMR (400 MHz, $CDCl_3$): $\delta$ = 0.77, 0.86, 1.12, 1.14, 1.16 (15H, s, 5× $CH_3$), 0.90 (3H, d, $J$ = 6.4 Hz, $CH_3$), 0.94 (3H, d, $J$ = 6.1 Hz, $CH_3$), 4.25 (2H, m, –$OCH_2$), 4.63 (2H, m, $CH_2ONO_2$), 5.28 (1H, t, $J$ = 7.0, 3.5 Hz, H-12), 7.27 (2H, d, $J$ = 5.8 Hz, 3', 5'-H), 7.38 (1H, s, =CHAr), and 8.64 (2H, d, $J$ = 5.0 Hz, 2', 6'-H) ppm; $^{13}C$ NMR (100 MHz, $CDCl_3$): $\delta$ = 15.6 (C29), 16.8 (C30), 17.2 (C23), 20.4 (C6), 21.2 (C24), 22.9 (C27), 23.5 (C26), 23.7 (C11), 24.2 (C22), 28.0 (C21), 29.6 (C25), 30.7 (C7), 32.2 (C16), 36.5 (C10), 36.7 (C15), 38.9 (C19), 39.2 (C20), 39.6 (C8), 42.4 (C17), 44.0 (C1), 45.3 (C18), 45.5 (C14), 48.5 (C4), 53.1 (C9), 53.3 (C5), 60.2 ($COOCH_2$), 70.6 ($CH_2ONO_2$), 124.2, (C3', C5'), 125.6 (C12), 134.2 (=CHAr), 138.0 (C4'), 138.2 (C13), 143.7 (C2), 150.0 (C2', C6'), 177.3 (C28), and 207.5 (C3) ppm; HRMS ($m/z$) $[M-H]^-$ calcd. for $C_{38}H_{51}N_2O_6$: 631.3753, found: 631.3744.

*2-[2-(4,6-Dimethoxypyrimidin-5-yl)vinyl]-3-oxo-urs-12-en-28-oic acid-(2-nitrooxy)ethyl ester (**5d**)*

Yellow-green solid; yield 88.2%; m.p. 105.7–106.2°C; IR (KBr): $\tilde{\nu}$ = 2953 (s), 2869 (w) (C–H, aliphatic), 1729 (s), 1680 (s) (2C=O), 1637 (vs) (C=C), 1565 (vs) (C=N, pyrimidinyl), and 1280 (vs) (C–O–C, ester) $cm^{-1}$; $^1H$ NMR (400 MHz, $CDCl_3$): $\delta$ = 0.77, 0.89, 1.08, 1.14, 1.16 (15H, s, 5× $CH_3$), 0.84 (3H, d, $J$ = 6.4 Hz, $CH_3$), 0.93 (3H, d, $J$ = 6.1 Hz, $CH_3$), 3.98 (6H, s, 2× $OCH_3$), 4.28 (2H, m, –$OCH_2$), 4.64 (2H, m, $CH_2ONO_2$), 5.24 (1H, t, $J$ = 6.8, 3.7 Hz, H-12), 7.24 (1H, d, $J$ = 2.5 Hz, 2'-H), and 8.41 (1H, s, =CHAr) ppm; $^{13}C$ NMR (100 MHz, $CDCl_3$): $\delta$ = 15.3 (C29), 16.9 (C30), 17.1 (C23), 20.3 (C6), 21.2 (C24), 21.2 (C27), 23.2 (C26), 23.5 (C11), 24.3 (C22), 28.0 (C21), 29.3 (C25), 30.7 (C7), 32.4 (C16), 36.3 (C10), 36.7 (C15), 38.9 (C19), 39.2 (C20), 39.6 (C8), 42.7 (C17), 43.8 (C1), 45.2 (C14), 45.6 (C18), 48.5 (C4), 53.1 (C9), 53.8 (C5), 54.4 (2×$OCH_3$), 60.2 ($COOCH_2$), 70.7 ($CH_2ONO_2$), 101.1 (C5'), 125.8 (C12), 127.3 (=CHAr), 137.6 (C13), 138.1 (C2), 156.5 (C2'), 167.6 (C4', C6'), 177.3 (C28), and 206.6 (C3) ppm; HRMS ($m/z$) $[M+H]^+$ calcd. for $C_{39}H_{56}N_3O_8$: 694.4062, found: 694.4059.

### 4.1.3 | General procedure for the preparation of compounds 6a–d

To a solution of compounds **5a–d** (1 eq.) in dry THF (25 ml) and absolute ethanol (5 ml), sodium borohydride (10 eq.) was added at 0°C. The mixture was stirred in the dark for 2 h. At the end of the reaction, 20 ml of distilled water was added and the pH was adjusted to 7 with 1 M hydrochloric acid. The mixture was then extracted with ethyl acetate (20 ml × 3), dried over anhydrous $MgSO_4$, and concentrated under reduced pressure. The crude product was purified

by silica gel column chromatography (PE/EtOAc, 25:1) to give corresponding pure compounds **6a**–**d**.

*2-[2-(Furan-2-yl)vinyl]-3β-hydroxy-urs-12-en-28-oic acid-(2-nitrooxy)ethyl ester (**6a**)*

Yellow solid; yield 66.4%; m.p. 198.4–198.9°C; IR (KBr): $\tilde{\nu}$ = 3557 (s) (–OH), 2926 (s), 2875 (s) (C–H, aliphatic), 1729 (vs) (C=O), 1643 (vs) (C=C), 1457 (s), 1488 (m) (C=C, furanyl), and 1277 (s) (C–O–C, ester) $cm^{-1}$; $^1$H NMR (400 MHz, $CDCl_3$): $\delta$ = 0.71, 0.74, 0.85 (9H, s, 3× C$\underline{H}_3$), 0.87 (3H, d, *J* = 6.44 Hz, C$\underline{H}_3$), 0.94 (3H, d, *J* = 6.20 Hz, C$\underline{H}_3$), 1.12 (6H, d, *J* = 2.08 Hz, 2× C$\underline{H}_3$), 2.24 (1H, d, *J* = 11.32 Hz, 18-H), 3.83 (1H, s, 3-H), 4.23–4.32 (2H, m, –OC$\underline{H}_2$), 4.65 (2H, dd, *J* = 3.96, 5.28 Hz, C$\underline{H}_2$ONO$_2$), 5.31 (1H, t, *J* = 3.36, 4.20 Hz, H-12), 6.23 (1H, d, *J* = 3.24 Hz, 3'-H), 6.37 (1H, dd, *J* = 3.24, 1.88 Hz, 4'-H), 6.44 (1H, s, =C$\underline{H}$Ar), and 7.35 (1H, d, *J* = 1.44 Hz, 5'-H) ppm; $^{13}$C NMR (100 MHz, $CDCl_3$): $\delta$ = 15.4 (C30), 15.7 (C29), 17.0 (C27), 17.1 (C25), 18.6 (C6), 21.3 (C24), 23.5 (C11), 23.7 (C23), 24.3 (C16), 28.1 (C21), 28.7 (C26), 30.7 (C1), 33.0 (C15), 36.7 (C22), 38.9 (C20), 39.2 (C19), 39.9 (C10), 40.7 (C8), 42.3 (C14), 43.0 (C7), 42.3 (C17), 46.9 (C9), 48.4 (C4), 53.0 (C18), 56.2 (C5), 60.2 (COO$\underline{C}$H$_2$), 70.7 (–$\underline{C}$H$_2$ONO$_2$), 81.3 (C3), 108.6 (C3'), 111.0 (C4'), 111.3 (=$\underline{C}$HAr), 125.9 (C12), 138.1 (C13), 140.0 (C2'), 141.4 (C5'), 153.5 (C2), and 177.4 (C28, C=O) ppm; HRMS (*m/z*) $[M+H]^+$ calcd. for $C_{37}H_{54}NO_7$: 624.3895, found: 624.3893.

*2-[2-(Thiophene-2-yl)vinyl]-3β-hydroxy-urs-12-en-28-oic acid-(2-nitrooxy)ethyl ester (**6b**)*

Pale-yellow solid; yield 81.8%; m.p. 182.5–182.8°C; IR (KBr): $\tilde{\nu}$ = 3555 (br) (–OH), 2924 (s), 2871 (s) (C–H, aliphatic), 1726 (s) (C=O), 1641 (vs) (C=C), 1454 (s), 1509 (m) (C=C, thiopheneyl), and 1279 (s) (C–O–C, ester) $cm^{-1}$; $^1$H NMR (400 MHz, $CDCl_3$): $\delta$ = 0.73 (6H, d, *J* = 5.12 Hz, 2× C$\underline{H}_3$), 0.87 (6H, d, *J* = 3.64 Hz, 2× C$\underline{H}_3$), 0.94 (3H, d, *J* = 6.12 Hz, C$\underline{H}_3$), 1.12 (6H, d, *J* = 5.88 Hz, 2× C$\underline{H}_3$), 2.23 (1H, d, *J* = 11.24 Hz, 18-H), 3.85 (1H, s, 3-H), 4.27 (2H, m, –OC$\underline{H}_2$), 4.64 (2H, m, C$\underline{H}_2$ONO$_2$), 5.31 (1H, t, *J* = 3.24, 3.40 Hz, H-12), 6.81 (1H, s, =C$\underline{H}$Ar), 6.98 (2H, d, *J* = 3.52 Hz, 3', 4'-H), and 7.19 (1H, t, *J* = 2.96, 3.48 Hz, 5'-H) ppm; $^{13}$C NMR (100 MHz, $CDCl_3$): $\delta$ = 15.4 (C30), 15.8 (C29), 17.0 (C27), 17.1 (C25), 18.5 (C6), 21.3 (C24), 23.5 (C11), 23.7 (C23), 24.2 (C16), 28.1 (C21), 28.8 (C26), 30.7 (C1), 33.0 (C15), 36.7 (C22), 38.9 (C20), 39.2 (C19), 39.9 (C10), 40.9 (C8), 42.3 (C14), 42.3 (C17), 43.3 (C7), 46.8 (C9), 48.4 (C4), 53.0 (C18), 56.2 (C5), 60.2 (COO$\underline{C}$H$_2$), 70.7 (–$\underline{C}$H$_2$ONO$_2$), 81.4 (C3), 115.8 (C3'), 124.1 (C4'), 125.9 (=$\underline{C}$HAr), 126.7 (C12), 127.8 (C5'), 138.1 (C13), 139.2 (C2'), 140.7 (C2), and 177.4 (C28, C=O) ppm; HRMS (*m/z*) $[M+H]^+$ calcd. for $C_{37}H_{54}NO_6S$: 640.3666, found 640.3617.

*2-[2-(Pyridin-4-yl)vinyl]-3β-hydroxy-urs-12-en-28-oic acid-(2-nitrooxy)ethyl ester (**6c**)*

White solid; yield 57.5%; m.p. 205.9–206.7°C; IR (KBr): $\tilde{\nu}$ = 3416 (br) (–OH), 2926 (s), 2871 (m) (C–H, aliphatic), 1727 (m) (C=O), 1638 (vs) (C=C), 1453 (w), 1545 (w), 1599 (m) (C=N, pyridinyl), and 1280 (s) (C–O–C, ester) $cm^{-1}$; $^1$H NMR (400 MHz, $CDCl_3$): $\delta$ = 0.69, 1.10, 1.15 (9H, s, 3× C$\underline{H}_3$), 0.76 (3H, d, *J* = 3.68 Hz, C$\underline{H}_3$), 0.84 (3H, d, *J* = 6.36 Hz, C$\underline{H}_3$), 0.93 (3H, d, *J* = 6.24 Hz, C$\underline{H}_3$), 2.20 (1H, d, *J* = 11.08 Hz, 18-H), 3.90 (1H, s, H-3), 4.24–4.27 (2H, m, –OC$\underline{H}_2$), 4.62–4.64 (2H, m, C$\underline{H}_2$ONO$_2$), 5.23 (1H, t, *J* = 6.8, 3.4 Hz, H-12), 6.69 (1H, s, =C$\underline{H}$Ar), 7.18 (2H, d, *J* = 5.56 Hz, 3', 5'-H), and 8.53 (2H, d, *J* = 4.88 Hz, 2', 6'-H) ppm; $^{13}$C NMR (100 MHz, $CDCl_3$): $\delta$ = 15.7 (C30), 15.9 (C29), 17.0 (C27), 17.1 (C25), 18.5 (C6), 21.3 (C24), 23.4 (C11), 23.6 (C23), 24.3 (C16), 28.0 (C21), 28.9 (C26), 30.7 (C1), 32.9 (C15), 36.8 (C22), 38.9 (C20), 39.2 (C19), 39.9 (C10), 40.6 (C8), 42.1 (C14), 42.2 (C7), 42.3 (C17), 47.0 (C9), 48.4 (C4), 52.9 (C18), 55.8 (C5), 60.2 (COO$\underline{C}$H$_2$), 70.6 (–$\underline{C}$H$_2$ONO$_2$), 81.0 (C3), 120.6 (C3'), 120.6 (C5'), 124.2 (C12), 125.5 (=$\underline{C}$HAr), 138.1 (C13), 145.4 (C4'), 147.5 (C2), 148.6 (C2'), 148.6 (C6'), and 177.3 (C28, C=O) ppm; HRMS (*m/z*) $[M+Na]^+$ calcd. for $C_{38}H_{54}N_2O_6Na$: 657.3874, found 657.3870.

*2-[2-(4,6-Dimethoxypyrimidin-5-yl)vinyl]-3β-hydroxy-urs-12-en-28-oic acid-(2-nitrooxy)ethyl ester (**6d**)*

White solid; yield 84.8%; m.p. 105.6–106.5°C; IR (KBr): $\tilde{\nu}$ = 3523 (br) (–OH), 2952 (vs), 2871 (s) (C–H, aliphatic), 1729 (s) (C=O), 1639 (vs) (C=C), 1567 (vs) (C=N, pyrimidinyl), and 1279 (s) (C–O–C, ester) $cm^{-1}$; $^1$H NMR (400 MHz, $CDCl_3$): $\delta$ = 0.62, 0.65, 0.78, 1.08, 1.13 (15H, s, 5× C$\underline{H}_3$), 0.84 (3H, d, *J* = 6.44 Hz, C$\underline{H}_3$), 0.93 (3H, d, *J* = 6.04 Hz, C$\underline{H}_3$), 2.18 (1H, d, *J* = 11.28 Hz, 18-H), 3.90 (1H, s, 3-H), 3.96 (6H, s, 2× OC$\underline{H}_3$), 4.24 (2H, dd, *J* = 3.32, 2.92 Hz, –OC$\underline{H}_2$), 4.61 (2H, t, *J* = 5.24, 4.00 Hz, –C$\underline{H}_2$ONO$_2$), 5.17 (1H, t, *J* = 3.40, 3.36 Hz, 12-H), 6.15 (1H, s, =C$\underline{H}$Ar), and 8.39 (1H, s, 2'-H) ppm; $^{13}$C NMR (100 MHz, $CDCl_3$): $\delta$ = 14.8 (C30), 15.8 (C29), 16.9 (C27), 17.1 (C25), 18.6 (C6), 21.2 (C24), 23.4 (C11), 23.7 (C23), 24.2 (C16), 28.0 (C21), 28.6 (C26), 30.7 (C1), 32.9 (C15), 36.7 (C22), 38.9 (C20), 39.2 (C19), 39.8 (C10), 39.9 (C8), 41.8 (C14), 42.2 (C17), 43.9 (C7), 47.0 (C9), 48.4 (C4), 52.8 (C18), 55.7 (C5), 60.2 (COO$\underline{C}$H$_2$), 70.6 (–$\underline{C}$H$_2$ONO$_2$), 81.1 (C3), 102.4 (C5'), 110.6 (C12), 125.7 (=$\underline{C}$HAr), 138.0 (C13), 144.4 (C2), 154.9 (C2'), 167.5 (C4'), 167.5 (C6'), and 177.3 (C28, C=O) ppm; HRMS (*m/z*) $[M+H]^+$ calcd. for $C_{39}H_{58}N_3O_8$: 696.4218, found 696.4217.

## 4.2 | Biological assays

### 4.2.1 | Cell lines and culture

Five human cancer cell lines consisting of the human lung cancer cell line A549, human breast cancer cell line MCF-7, human liver cancer cell line HepG-2, human colon cancer cell line HT-29, and the human cervical cancer cell line HeLa were purchased from the Shanghai Institute of Biochemistry and Cell Biology (China). Cell lines were cultured in RPMI 1640 medium supplemented with 10% FBS at 37°C in a humidified 5% $CO_2$ atmosphere. The medium was refreshed every 2 days and the growth of cells was monitored regularly under the inverted microscope.

### 4.2.2 | MTT assay

The tested tumor cell lines were harvested and seeded at a density of $1 \times 10^3$ cells/well into 96-well plates. After 24 h of incubation in a

humidified atmosphere with 5% $CO_2$ at 37°C, the cells were exposed to various concentrations of compounds **5a–d** and **6a–d** in a medium containing 0.1% DMSO for 48 h. Then, 10 μl of MTT (5 mg/ml, in phosphate-buffered saline [PBS]) was added to each well. Next, the cells were incubated for another 4 h. The supernatant was discarded and 150 μl of DMSO was added to dissolve the formazan. The absorbance was determined at 490 nm by a Multiskan FC Microplate Reader (Thermo Fisher Scientific). The $IC_{50}$ value was calculated by GraphPad Prism Software. Negative control (cells+medium), blank control (only medium), and positive control (cisplatin) were co-assayed.

### 4.2.3 | AO/EB and DAPI staining

MCF-7 cells were harvested ($2 \times 10^4$ cells/well) and incubated in 6-well plates overnight. The cells were treated with indicated concentrations of compound **5c** for 24 h. After treatment, the cells were washed three times with PBS. Next, 500 μl of 1 × dilution buffer containing 20 μl of a 1:1 (v/v) AO/EB mixture was added to the cells. Then the cells were stained with AO/EB for 5 min at room temperature in the dark, and 5 μl of cell suspension was transferred to a sterile glass slide and covered with a coverslip. The morphology of cells was imaged using a fluorescence microscope (Olympus) with 488-nm excitation and 525-nm emission.

Cells treatment of DAPI staining was similar to that of AO/EB staining. After washing with PBS three times, MCF-7 cells were stained with 1 ml of 300 nM DAPI in PBS for 20–30 min at 37°C. Subsequently, the cells were collected, washed twice by PBS, and resuspended in 1 ml of PBS. Next, 5 μl of cell suspension was transferred to a sterile glass slide and covered with a coverslip. The morphology of cells was investigated using a fluorescence microscope.

### 4.2.4 | Apoptosis assay (annexin V-FITC/PI)

MCF-7 cells were harvested ($2 \times 10^4$ cells/well) and incubated in six-well plates overnight. After treatment with indicated concentrations of compound **5c** for 24 h, MCF-7 cells were washed twice with PBS and collected by centrifugation. The resulting cells were then resuspended in 1× incubation buffer and incubated with annexin V-FITC/PI kit (Dalian Meilun Biotech) in the dark at room temperature for 15 min. The fluorescent signal was detected by the FACSCanto II flow cytometer (BD Biosciences).

### 4.2.5 | Cell cycle analysis

After being harvested and seeded in six-well plates ($2 \times 10^4$ cells/well), MCF-7 cells were treated with indicated concentrations of compound **5c** for 24 h. The cells were washed with PBS, collected by centrifugation at 1000 r/min for 5 min, and fixed in 70% ethanol at 4°C overnight. Next, the cells were centrifuged (1000 r/min, 3 min), washed with PBS, and resuspended with 50 μg/ml PI and 0.1 mg/ml RNase A for 30 min at room temperature. Cell cycle analysis was performed on the FACSCanto II flow cytometer (BD Biosciences).

### 4.2.6 | Membrane potential detection

MCF-7 cells were harvested ($2 \times 10^4$ cells/well) and incubated in 6-well plates overnight. Then, the cells were treated with indicated concentrations of compound **5c** for 24 h. After treatment, the cells were washed with PBS, resuspended in 500 μl of culture medium, and incubated with 10 μg/ml JC-1 for 20 min. Immediately after centrifugation at 600*g* for 4 min, the cells were rinsed twice with 1× incubation buffer. JC-1 fluorescence was determined by the FACSCanto II flow cytometer (BD Biosciences).

### 4.2.7 | ROS detection

MCF-7 cells were harvested ($2 \times 10^4$ cells/well) and incubated in 6-well plates overnight. The cells were treated with indicated concentrations of compound **5c** for 24 h. Thereafter, the medium was removed, the cells were washed with PBS, and collected by centrifugation (1000 r/min, 5 min). Then, 10 μM of DCFH-DA was added to the cells and incubated for 20 min at 37°C. Finally, the cells were washed three times in a serum-free medium and resuspended in PBS. The generation of ROS was measured with excitation at 488 nm and emission at 525 nm by the FACSCanto II flow cytometer (BD Biosciences).

### 4.2.8 | Western blot

MCF-7 cells were seeded ($1 \times 10^6$ cells/dish) in 60-mm culture dishes. After overnight incubation, the cells were treated with indicated concentrations of compound **5c** for 24 h. The cells were lysed with an ice-cold radioimmunoprecipitation assay containing 1 mM phenylmethylsulfonyl fluoride for 30 min. The mixture was centrifuged at $1.2 \times 10^5$ r/min at 4°C for 10 min. Then, loading buffer was added to the supernatant and the samples were treated in boiling water for 5 min, and 5 μl of protein samples were separated by 12% sodium dodecyl sulfate-polyacrylamide gel electrophoresis and then transferred to a polyvinylidene fluoride (PVDF) membrane. The PVDF membrane was blocked by 5% nonfat powdered milk and washed three times with Tris-buffered saline and Tween 20 (TBST) (10 min/time). After overnight incubation at 4°C in the primary antibody diluted with TBST, the membrane was washed with TBST. A secondary antibody, containing 5% nonfat powdered milk was added, the membrane was incubated for 1 h at room temperature, and then the membrane was washed with PBST (phosphate-buffered saline with Tween 20) again. The relative protein band was detected using enhanced chemiluminescence Western blot analysis substrate with Chemiluminescent Imaging System (Tanon).

### 4.2.9 | Statistical analysis

The data are presented as the mean ± standard deviation. No statistical method was used for data analysis.

## 4.3 | Docking methodology

SYBYL-X 2.0.0 software (Tripos) was used to assess the interaction between compound **5c** and caspase 8 (PDB: 2c2z, www.rcsb.org). Briefly, the ligand, water molecules, and cofactors were removed from the protein. The structure of compound **5c** was created by using Chemoffice (PerkinElmer). The MM2 force field was used for energy minimization of ligands using Docking Server. Compound **5c** was docked into the active site of caspase 8 using the flexible docking method. Typical parameters including total score, crash value, and polar score were calculated to predict protein–ligand interaction. Results of binding were also analyzed by Discovery Studio (BIOVIA).

## ACKNOWLEDGMENTS

This study was supported by start-up funding for postdoctoral research from Guangzhou University of Chinese Medicine (AFD01820Z0373).

## CONFLICTS OF INTEREST

The authors declared that there are no conflicts of interest.

## ORCID

*Jiamei Lei* https://orcid.org/0000-0001-8224-5682

## REFERENCES

[1] Y. Fuchs, H. Steller, *Nat. Rev. Mol. Cell Biol.* **2015**, *16*, 329.
[2] S. Webb, D. Harrison, A. H. Wyllie, *Adv. Pharmacol.* **1997**, *41*, 1.
[3] J. C. Rathmell, C. B. Thompson, *Cell* **2002**, *109*, 97.
[4] D. A. Carson, J. M. Ribeiro, *Lancet* **1993**, *341*, 1251.
[5] A. Breindl, *Bioworld Today* **2008**, *19*, 1.
[6] Z. F. Zhu, C. Chen, J. X. Jiang, Q. Z. Zhang, Z. B. Du, S. X. Wei, X. H. Song, J. Tang, J. P. Lei, Z. F. Ke, Y. Zou, *Org. Chem. Front.* **2020**, *7*, 1122.
[7] K. Kobayashi, H. Hatano, M. Otaki, T. Ogasawara, T. Tokuhisa, *Proc. Natl. Acad. Sci. USA* **1999**, *96*, 1457.
[8] W. Wick, S. Wagner, S. Kerkau, J. Dichgans, J. C. Tonn, M. Weller, *FEBS Lett.* **1998**, *440*, 419.
[9] M. O. Hengartner, *Nature* **2000**, *407*, 770.
[10] T. J. Fan, L. H. Han, R. S. Cong, J. Liang, *Acta Biochim. Biophys. Sin.* **2005**, *37*, 719.
[11] E. C. D. Bruin, D. Meersma, J. D. Wilde, I. D. Otter, E. M. Schipper, J. P. Medema, L. T. C. Peltenburg, *Cell Death Differ.* **2003**, *10*, 1204.
[12] M. Fritsch, S. D. Günther, R. Schwarzer, M. C. Albert, F. Schorn, J. P. Werthenbach, L. M. Schiffmann, N. Stair, H. Stocks, J. M. Seeger, M. Lamkanfi, M. Krönke, M. Pasparakis, H. Kashkar, *Nature* **2019**, *575*, 683.
[13] M. Donepudi, A. M. Sweeney, C. Briand, M. G. Grütter, *Mol. Cell* **2003**, *11*, 543.
[14] C. Ma, S. H. MacKenzie, A. C. Clark, *Prot. Sci.* **2014**, *23*, 442.
[15] K. Jakubowska, K. Guzińska-Ustymowicz, W. Famulski, D. Cepowicz, D. Jagodzińska, A. Pryczynicz, *Oncol. Lett.* **2016**, *11*, 1879.
[16] N. A. Agalakova, T. I. Petrova, G. P. Gusev, *J. Evol. Biochem. Physiol.* **2019**, *55*, 97.
[17] R. Mandal, J. Compte, I. Kostova, S. Becker, K. Strebhardt, *Biochim. Biophys. Acta, Rev. Cancer* **2020**, *1873*, 188357.
[18] R. E. D. Angel, S. M. Smith, R. D. Glickman, S. N. Perkins, S. D. Hursting, *Nutr. Cancer* **2010**, *62*, 1074.
[19] L. S. Bergamin, F. Figueiró, F. Dietrich, F. D. M. Manica, E. C. Filippi-Chiela, F. B. Mendes, E. H. F. Jandrey, D. V. Lopes, F. H. Oliveira, I. C. Nascimento, H. Ulrich, A. M. O. Battastini, *Eur. J. Pharmacol.* **2017**, *811*, 268.
[20] T. Tian, X. Liu, E. Lee, J. Sun, Z. Feng, L. Zhao, C. Zhao, *Arch. Pharm. Res.* **2017**, *40*, 458.
[21] Y. Q. Meng, C. D. Xu, T. T. Yu, W. Li, Q. W. Li, X. X. Li, *J. Asian Nat. Prod. Res.* **2020**, *22*, 359.
[22] W. Wang, R. Liu, Z. Baloch, *Oncol. Lett.* **2018**, *15*, 2323.
[23] J. W. Shao, Y. C. Dai, J. P. Xue, J. C. Wang, F. P. Lin, Y. H. Guo, *Eur. J. Med. Chem.* **2011**, *46*, 2652.
[24] S. S. Wang, Q. L. Zhang, P. Chu, L. Q. Kong, G. Z. Li, Y. Q. Li, L. Yang, W. J. Zhao, X. H. Guo, Z. Y. Tang, *Bioorg. Chem.* **2020**, *101*, 104036.
[25] O. O. Kolomoitsev, V. M. Kotliar, D. O. Tarasenko, O. V. Buravov, A. O. Doroshenko, *Monatsh. Chem.* **2020**, *151*, 765.
[26] B. A. Dar, A. M. Lone, W. A. Shah, M. A. Qurishi, *Eur. J. Med. Chem.* **2016**, *111*, 26.
[27] H. Zhou, Y. Dong, X. Ma, J. Xu, S. Xu, *Fitoterapia* **2020**, *146*, 104670.
[28] S. V. Vasilieva, M. S. Petrishcheva, E. I. Yashkina, A. N. Osipov, *Mol. Biol. Rep.* **2019**, *46*, 719.
[29] T. Zhang, B. He, H. Yuan, G. Feng, F. Chen, A. Wu, L. Zhang, H. Lin, Z. Zhuo, T. Wang, *Chem. Biodivers.* **2019**, *16*, e1900111.
[30] S. Ceylan, H. Bektas, H. Bayrak, N. Demirbas, S. Alpay-Karaoglu, S. Ulker, *Arch. Pharm. (Weinheim, Ger.).* **2013**, *346*, 743.
[31] Y. Shen, J. Li, S. Chen, J. Wan, Y. B. Zhao, Z. H. Lu, M. Li, L. Yang, X. Yu, D. Chen, Z. Pan, *ChemistrySelect* **2017**, *2*, 11206.
[32] V. Venepally, R. C. R. Jala, *Eur. J. Med. Chem.* **2017**, *141*, 113.
[33] H. A. E. Mohamed, H. F. Al-Shareef, *Anti-Cancer Agents Med. Chem.* **2019**, *19*, 1132.
[34] S. Radi, S. Tighadouini, O. Feron, O. Riant, M. Bouakka, R. Benabbes, Y. N. Mabkhot, *Molecules* **2015**, *20*, 20186.
[35] R. M. Mohareb, F. M. Manhi, M. A. A. Mahmoud, A. Abdelwahab, *Med. Chem. Res.* **2020**, *29*, 1536.
[36] L. Huang, R. Huang, F. Pang, A. Li, G. Huang, X. Zhou, Q. Li, F. Li, X. Ma, *RSC Adv.* **2020**, *31*, 18008.
[37] F. Garbin, K. Eckert, H. R. Maurer, *J. Immunol. Methods* **1994**, *170*, 269.
[38] G. Jiao, X. He, X. Li, J. Qiu, H. Xu, N. Zhang, S. Liu, *RSC Adv.* **2015**, *5*, 53240.
[39] C. Downey, D. H. Craig, M.D. Basson, *Am. J. Surg.* **2011**, *202*, 520.
[40] I. K. Kim, R. L. Copeland, Jr. J. H. Lee, H. S. Kim, E. Asafo-Adjei, N. D. Brown, J. S. Estrada, R. K. Gordon, G. E. Garcia, P. K. Chiang, *J. Biomed. Sci.* **1994**, *1*, 154.
[41] Y. S. Takano, B. V. Harmon, J. F. Kerr, *J. Pathol.* **1991**, *163*, 329.
[42] N. Atale, S. Gupta, U. C. S. Yadav, V. Rani, *J. Microsc.* **2014**, *255*, 7.
[43] D. W. Li, G. R. Li, Y. Lu, Z. Q. Liu, M. Chang, M. Yao, W. Cheng, L. S. Hu, *Int. J. Mol. Med.* **2013**, *32*, 108.
[44] J. H. Reed, P. J. Neufing, M. W. Jackson, R. M. Clancy, P. J. Macardle, J. P. Buyon, T. P. Gordon, *Clin. Exp. Immunol.* **2007**, *148*, 153.
[45] M. Fussenegger, J. E. Bailey, *Biotechnol. Prog.* **1998**, *14*, 807.
[46] D. L. Myster, R. J. Duronio, *Curr. Biol.* **2000**, *10*, 302.
[47] S. Risal, D. Adhikari, K. Liu, *Methods Mol. Biol.* **2016**, *1336*, 155.
[48] K. Vermeulen, D. R. V. Bockstaele, Z. N. Berneman, *Cell. Prolif.* **2003**, *36*, 131.
[49] B. K. Bhuyan, L. G. Scheidt, T. J. Fraser, *Cancer Res.* **1972**, *32*, 398.
[50] E. Sugikawa, T. Hosoi, N. Yazaki, M. Gamanuma, N. Nakanishi, M. Ohashi, *Anticancer Res.* **1999**, *19*, 3099.

[51] R. Katrina, *Nat. Rev. Gastroenterol. Hepatol.* **2015**, *12*, 428.
[52] J. D. Ly, D. R. Grubb, A. Lawen, *Apoptosis* **2003**, *8*, 115.
[53] J. M. Jürgensmeier, J. Panse, R. Schäfer, G. Bauer, *Int. J. Cancer* **1997**, *70*, 587.
[54] B. Giuseppina, *ISRN Oncol.* **2012**, *10*, 137289.
[55] H. E. G. Ghaleh, L. Zarei, B. M. Motlagh, N. Jabbari, *Artif. Cells Nanomed. Biotechnol.* **2019**, *47*, 1396.
[56] R. Malla, S. Gopinath, K. Alapati, C. S. Gondi, M. Gujrati, D. H. Dinh, S. Mohanam, J. S. Rao, *PLOS One* **2010**, *5*, e13731.
[57] D. Javelaud, F. Besancon, *J. Biol. Chem.* **2002**, *277*, 37949.
[58] R. Kim, M. Emi, K. Tanabe, *Cancer Chemother. Pharmacol.* **2006**, *57*, 545.
[59] I. H. Engels, A. Stepczynska, C. Stroh, K. Lauber, C. Berg, R. Schwenzer, H. Wajant, R. U. Jänicke, A. G. Porter, C. Belka, M. Gregor, K. Schulze-Osthoff, W. Wesselborg, *Oncogene* **2000**, *19*, 4563.

**How to cite this article:** B. He, Z. Zhu, F. Chen, R. Zhang, W. Chen, T. Zhang, T. Wang, J. Lei, *Arch. Pharm.* **2021**, e2000448.